c1

APPLICATION OF A NEW TECHNIQUE TO THE MEASUREMENT OF STARK SHIFTS

by

EDWIN GEORGE THIESSEN

B. Sc., University of Saskatchewan, 1969

A THESIS SUBMITTED IN PARTIAL FULFILMENT OF THE REQUIREMENTS FOR THE DEGREE OF MASTER OF SCIENCE

in the Department

of

PHYSICS

We accept this thesis as conforming to the required standard

THE UNIVERSITY OF BRITISH COLUMBIA

April, 1973

In presenting this thesis in partial fulfilment of the requirements for an advanced degree at the University of British Columbia, I agree that the Library shall make it freely available for reference and study. I further agree that permission for extensive copying of this thesis for scholarly purposes may be granted by the Head of my Department or by his representatives. It is understood that copying or publication of this thesis for financial gain shall not be allowed without my written permission.

Department of Physics

The University of British Columbia
Vancouver 8, Canada

Date April 19, 1973

ABSTRACT

A variation of the classical canal ray source has been developed for the study of the Stark Effect in positive ion lines. Stress was placed on the measurement of small line shifts rather than the attainment of large electric fields. To this end a sensitive shift measuring apparatus employing a linear neutral density filter to translate the line shift into a change in intensity was built.

Shifts were measured to an accuracy of about .02 A^{o} in the following lines: He I 5016 A^{o}, 7281 A^{o}, 6678 A^{o}, 3889 A^{o} and Ar I 4272 A^{o}, 4266 A^{o}. No shifts were detected in Ar II 4727 A^{o} and 4806 A^{o}.

A discussion of prospective improvements to be made in the apparatus is also included. With these improvements, the apparatus should be capable of measuring shifts to an accuracy of .001 A^{o}.

TABLE OF CONTENTS

LIST OF FIGURES

LIST OF TABLES

ACKNOWLEDGEMENTS

I wish to thank my supervisor, Dr. A.J. Barnard, for his helpful comments during the course of this experiment and for his patient assistance during the writing of the thesis.

I would also like to thank other members of the group, particularly Dr. B. Ahlborn, Dr. J. Meyer, and Dr. R. Morris, for stimulating discussions held with them during the course of this work.

I would like to express my appreciation to Messrs. D. Sieberg and J. Zangeneh for their help in the electronics design and Mr. J. Bosma for his help during the design of the Stark source and wedge apparatus.

Yielding to threats of marital tumult, I hereby acknowledge typing and editorial assistance rendered by J. Thiessen.

Financial assistance from the National Research Council of Canada is gratefully acknowledged.

Chapter One

INTRODUCTION

1.1 Historical Introduction*

The effect of an external electric field on atomic spectra was discovered by Stark in experiments done on hydrogen in 1913. In the same year, Bohr developed his theory of the atom but it was not until 1916 that Schwarzschild and Epstein, working independently, explained the splitting of the hydrogen lines using the Bohr theory. The Stark effect was also the first application of Schroedinger's wave mechanics theory. This work was done independently by Schroedinger and Epstein in 1926.

Two years after Stark's discovery, Koch observed the Stark effect in the two electron system of helium. In He, however, the effect was much more complicated, with lines being shifted to smaller and larger wavelengths with and without splitting into polarized components. Also in many-electron systems, the selection rules involving $\Delta \ell$ were broken in the presence of an electric field. Bohr could explain some aspects of the He spectrum using

* All historical information up to 1939 comes from a review article by Verleger (1939).

eccentric orbits but a more accurate description was left to Schroedinger's wave mechanics and later to Dirac's theory of quantum mechanics.

Between the two world wars research on the Stark effect was extremely active with many improvements being made in theoretical and experimental aspects of the problem. Both the canal ray and Lo Surdo types of sources were improved by various authors and the field strength was pushed further up. In 1930 von Traubenburg and Gebauer attained a field of 1100 kV/cm and in 1936 Bomke attained a field of 1300 kV/cm.

For the purposes of this experiment it is interesting to note the work done on helium and argon during this period. Foster, between 1924 and 1936, did a fairly exhaustive study of He both theoretically and experimentally. Ryde, beginning in 1932, studied the Stark effect in about 160 lines of Ar from 8000 - 4200 A^{o} in fields from 55 to 155 kV/cm.

During the Second World War, there was very little activity on the Stark effect. After the war, further work was immediately begun, but most of the interest was in more complex molecular systems. The only immediate postwar work of interest in this experiment is that done by Minnhagen, who, in 1948, studied about 80 lines in the visible Ar II

spectrum and measured shifts on 20 of them. Measurements of the shifts of a few He I lines were also included in this paper. In 1949 he measured numerous levels of Ar I, correcting some of the earlier work of Foster and Horton.

In the 1950's, Stark broadening measurements on plasma lines began to be popular and this work has been a major factor in the recent revival of interest in the Stark effect in atoms. Bonch-Bruevich and Khodovoi (1967) have written a review paper on the most recent methods used in Stark effect experiments.

1.2 Theory

The theory for the Stark effect has been well known for years, but a brief summary of it is presented here as this will lead easily into the reasons why further work on the effect is important. The notation used will be the same as that in Condon and Shortley (1951).

Consider a transition between two levels with angular momentum quantum numbers J,M and J_o,M_o. J',M' are the same quantum numbers for one of the levels lying close to the upper level J,M.

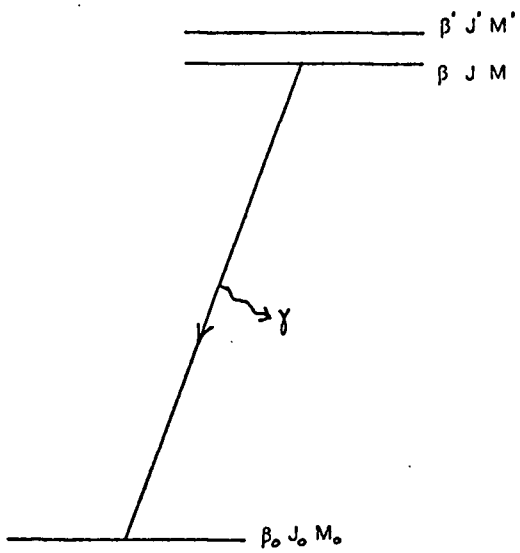

Figure 1. Theoretical Transition Considered

The hamiltonian of the atom in the electric field is

$$H = H_o + e\mathcal{E}z$$

where H_o is the hamiltonian in zero field, and
$\mathcal{E}$ is the electric field (which is in the z - direction).

It will be assumed that the shift of the lower level is negligible in comparison to the upper level shift so that the change in transition energy from the state $|\beta J M\rangle$ to the state $|\beta_o J_o M_o\rangle$ is given by the shift in the upper level. From standard perturbation theory, if one assumes $|\Delta E| \ll |E_{\beta J} - E_{\beta' J'}|$, the first order change in the

energy is given by

$$\langle \beta J M | e \mathcal{E} z | \beta J M \rangle = 0$$

since $e\mathcal{E}z$ is odd.

The second order perturbation is

$$\Delta E = \sum_{J' \neq J} \frac{|\langle \beta J M | e \mathcal{E} z | \beta' J' M' \rangle|^2}{E_{\beta J} - E_{\beta' J'}}$$

$$= \sum_{J' \neq J} \begin{pmatrix} J & J' & 1 \\ M & M & 0 \end{pmatrix}^2 \frac{e^2 \mathcal{E}^2 |\langle \beta J \| r \| \beta' J' \rangle|^2}{E_{\beta J} - E_{\beta' J'}}$$

where $\langle \beta J \| r \| \beta' J' \rangle$ is the reduced matrix element.

For the case of a particular atom, further assumptions can usually be made. For example, in the case of He, LS coupling can be assumed and the reduced matrix element becomes

$$\langle \alpha L S J \| r \| \alpha' L' S' J' \rangle$$

$$= \begin{Bmatrix} S & J & J' \\ 1 & L' & L \end{Bmatrix} \delta_{SS'} \langle \alpha L \| r \| \alpha' L' \rangle (2J+1)(2J'+1)$$

Assuming that the atom consists of a core plus

an optical electron, we can write

$$\alpha L = \gamma L^I S^I \ell L$$

and

$$\langle \alpha L \| r \| \alpha' L' \rangle$$

$$= \delta_{S^I S^{I'}} \delta_{L^I L^{I'}} \begin{Bmatrix} L^I & L & L' \\ 1 & \ell & \ell' \end{Bmatrix} \langle \ell \| r \| \ell' \rangle (2L+1)(2L'+1)$$

Going back to the expression for ΔE, we now have

$$\Delta E(J,M) = \mathcal{E}^2 \sum{}' \begin{pmatrix} J & J' & 1 \\ M & M & 0 \end{pmatrix}^2 \begin{Bmatrix} S & J & J' \\ 1 & \ell & \ell' \end{Bmatrix}^2 \begin{Bmatrix} L^I & L & L' \\ 1 & \ell & \ell' \end{Bmatrix} (2L+1)(2L'+1)$$

$$\times \ell_> (2\ell+1)(2\ell'+1) \frac{\sigma^2_{n\ell n'\ell'}}{E_{\beta J} - E_{\beta J'}}$$

where $\sum'$ indicates a sum over all primed quantum numbers and $\ell_>$ is the largest of ℓ and ℓ'.

$\sigma^2_{n\ell n'\ell'}$ depends on the radial wave functions and is given by

$$\sigma^2_{n\ell n'\ell'} = \left| \int r\, R_{n\ell}\, R_{n'\ell'}\, dr \right|^2 \frac{1}{(2\ell'+1)(2\ell+1)}$$

The above calculation was done for the special case of He, but for other atoms, by making other assumptions, the expression for ΔE may be reduced to a similar expression involving other radial functions.

If there is only one close by level, J',M', dominating the shift of the J,M level, the sum reduces to one term and we get a value for $\sigma^2_{n\ell n'\ell'}$. This value can be used in Stark broadening calculations and as a check on the radial wave function $R_{nl}(r)$ using

$$\sigma^2_{n\ell n'\ell'} = \left| \int r\, R_{n\ell}\, R_{n'\ell'}\, dr \right|^2 \frac{1}{(2\ell'+1)(2\ell+1)}$$

These σ^2 functions are usually obtained in the Coulomb approximation.

1.3 Present Work

We are now at the stage where a rationale for the present work can be put forward.

In the previous work done by Minnhagen (1948), the shifts of some Ar I and Ar II lines were measured. If these shifts are compared with theoretical values obtained

using σ^2 in the Coulomb approximation, the agreement is often poor. Yet these same σ^2's are used with the utmost of confidence in Stark broadening calculations. A systematic check of all the σ^2 values used in these calculations is obviously required, but in order to do this, Stark shifts of a large number of lines need to be accurately measured. Minnhagen has measured some of the levels required but the levels with the smaller shifts could either not be measured at all by him or were measured inaccurately.

Thus a more accurate determination of the smaller Stark shifts of many Ar II lines is in order and this is the objective of the present experiment. The technique used is a new one developed by R. Morris (1972) and consists of placing a linear neutral density filter in the exit plane of a monochromator. The line to be measured is placed on the centre of this linear "transmission wedge" and when the high field is applied to the atoms, the shift of the line is translated into a change in intensity. This technique is capable of resolving smaller line shifts than the simpler method of measuring the actual shifts of the lines.

Chapter Two

APPARATUS

The apparatus required to measure the small Stark shifts of many Ar II lines consists, broadly speaking, of a light source and a data acquisition system. The light source is an apparatus which produces a beam of positive ions in a high electric field. The details of the design and construction of this source are presented in section 2.1.

The data acquisition system is described in section 2.2. It consists of a lens system to gather the light from the ion beam, a monochromator and wedge apparatus to translate the line shift into a change in intensity, and a photon counting electronics system to measure the intensity change.

2.1 Ion Beam and High Field System

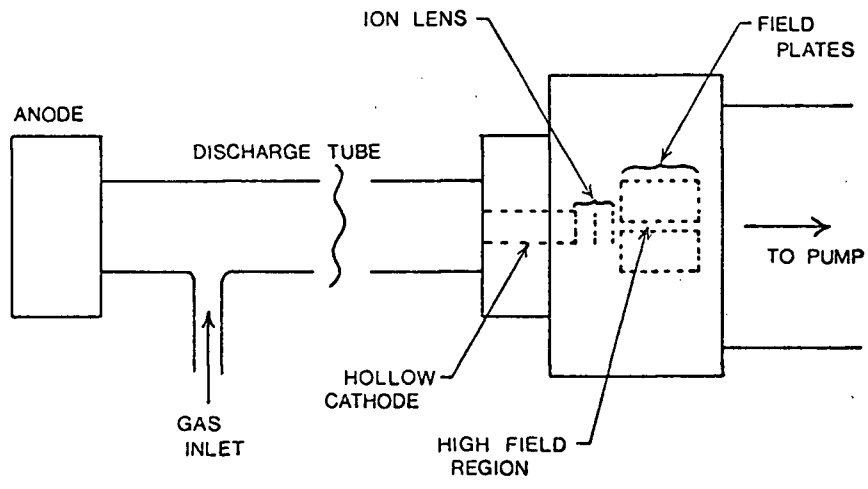

Figure 2. Schematic of Ion Beam and High Field System

The section of the apparatus which produces the positive ions in the high electric field consists of a hollow cathode discharge tube in which the ions are produced, an ion accelerating lens which extracts the ions through a slit in the end of the cathode, and a high field region into which the ion beam is shot. Gas is continuously pumped from the inlet in the discharge tube, through the slit in the hollow cathode, into the high field region and from there, out of the system.

2.1.1 Hollow Cathode Ion Source

The ion source (see Fig. 3) consists of a water cooled aluminum anode and cathode separated by a pyrex discharge tube about 50 cm long and 3.0 cm in diameter. The cathode, instead of being plane, has a hole of 10 mm diameter in it and into this hole is pushed a cylindrical aluminum insert of I.D. 7/32 in. This insert must be cleaned or even replaced periodically due to heavy pitting by the discharge. The plane face of the cathode is covered by a lava cylinder, as shown in Fig. 3, to prevent sputtering of the aluminum by ion bombardment.

Gas is leaked into the discharge tube near the anode and flows out through a slit at the base of the hollow cathode insert. The discharge between anode and grounded cathode is run at about 400 volts and 45 mA in a pressure of about 1 Torr. A ballast resistor of 25 KΩ and 225 watts is in series with the discharge tube to provide some current stability.

The diameter and length of the hollow cathode was determined partly by trial and error and partly by reference to previous authors (Mark and Wierl (1929), Thornton (1935), Foster and Snell (1937), Ryde (1938), Ryde (1942), Maissel (1958), Steubing and Schaeder (1936)). The approximate size was determined by consulting previous authors and then

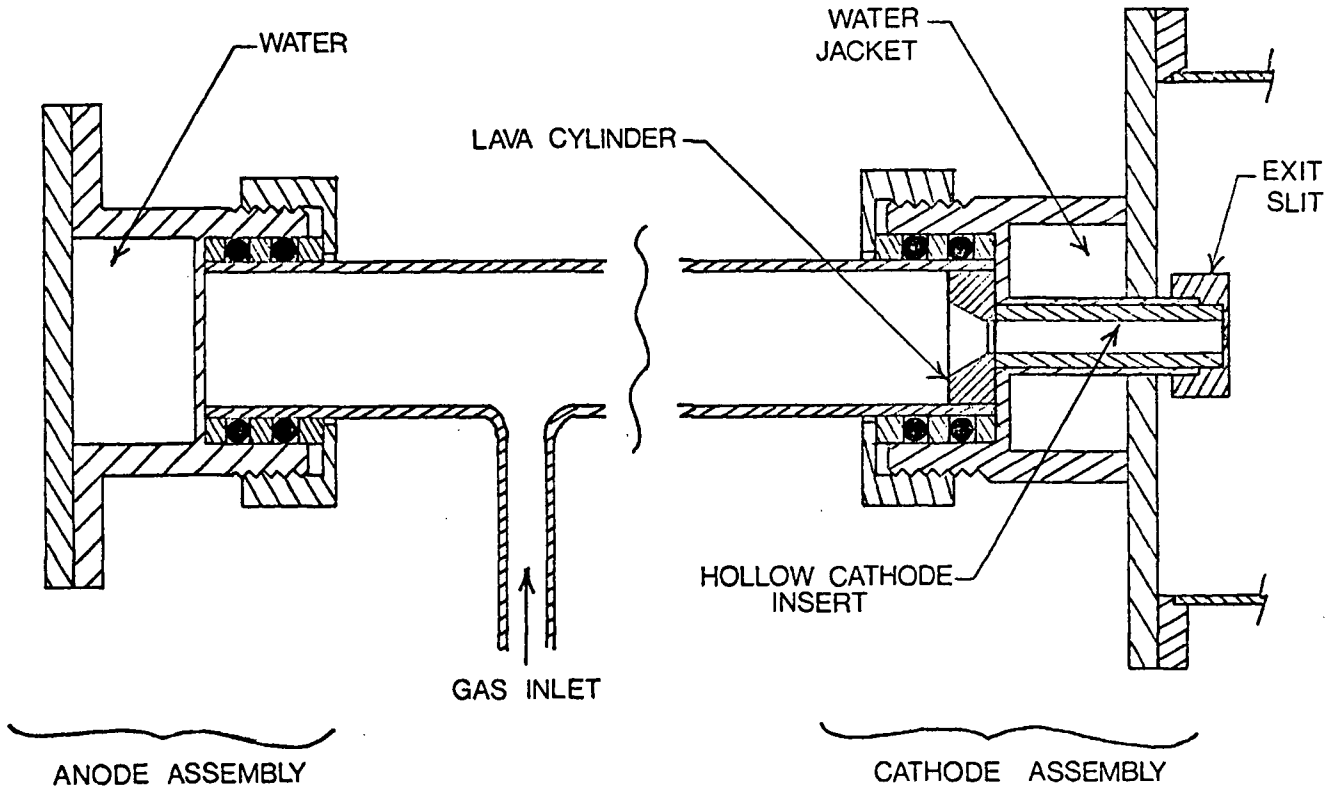

Figure 3. Detailed Assembly of Hollow Cathode Ion Source

inserts of different I.D.'s were used until the brightness of the discharge in the hollow cathode and intensity of ions from it were maximized.

2.1.2 Ion Accelerating Lens

All previous authors who used the canal ray method placed a slit at the end of the hollow cathode and the emerging beam of ions and neutrals was strong enough for them to study the Stark effect in the neutral atoms. Most of these authors do not give details of exposure times and films used, so it is difficult to know how intense their beams were.

This experiment was first attempted with simply a slit at the end of the hollow cathode. A fairly bright beam was obtained before the Stark field plates were put into place, but with the plates in place, only a dim glow was seen between them. To solve this problem, an ion lens was inserted between the hollow cathode and the field plates. The lens used is a simple three element electrostatic lens similar to the type used in the Nier Gun mass spectrometer ion source. The theory for this lens is described by Barnard (1953) and is summarized below.

The lens consists of three plates, A, B, and C, at 0 volts, V_1, and V_2. The separations between the plates are d_1 and d_2 as shown in Fig. 4.

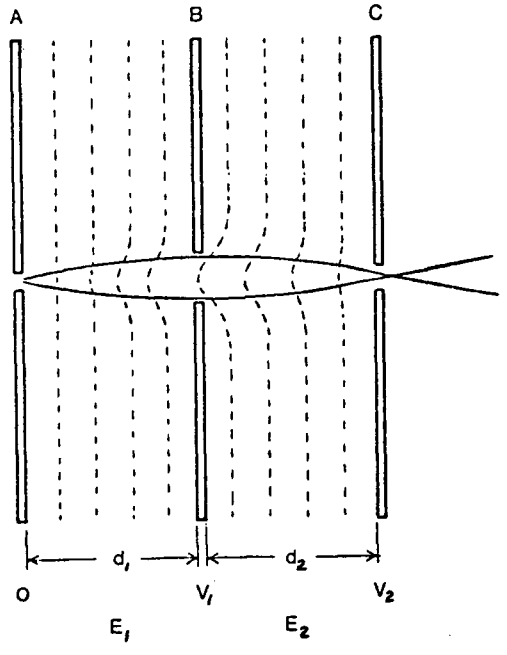

Figure 4. Ions Lens Schematic

The voltages V_1 and V_2 are set such that the field E_2 in the second region is larger than the field E_1 in the first. Equipotential surfaces from the region BC then bulge into the region AB as shown. Ions drawn from the left of plate A hit these equipotential lines at an acute angle and their path is bent towards the axis of the lens. The object of the lens is to accelerate the beam coming through the slit in A and focus it on the slit in C.

The focal length of the lens is given by

$$\frac{1}{f} = \frac{1}{d_1} + \frac{1}{d_2} = \frac{E_2 - E_1}{2V_1}$$

In this expression, the following assumptions have been made:

(i) the slit width is small in relation to the plate separation;

(ii) the slit is infinitely long;

(iii) the plates are thin with respect to the slit width;

(iv) the ions begin with zero kinetic energy; and

(v) space charge effects are neglected.

If $d_1 = d_2$, the relation between V_1 and V_2 to have the ions focus on the exit slit in plate C is $V_2 = 6\ V_1$.

For the lens used in this experiment, $d_1 = d_2 = .120$ in. The voltage V_2 was made as high as possible (8 kV) so that the ions would get as far as possible into the high field region between the Stark plates before hitting the negative plate.

The lens is shown in Fig. 5. It consists of the exit slit fastened to the end of the hollow cathode using set screws and two .025 in thick stainless steel plates held to the exit slit by two nylon screws protruding from it. These screws pass through the centre plate and thread into two round nuts spot welded to the end plate. The plates are kept apart by baked lava spacers which have been threaded on the outside to increase the tracking distance between the plates. The spacers between the centre and end plates come

up around the nuts, again to increase the tracking distance. Smooth unbaked lava spacers were used at first, but these tracked very badly when they became only slightly dirtied by the beam. The baked threaded spacers take much longer before tracking occurs.

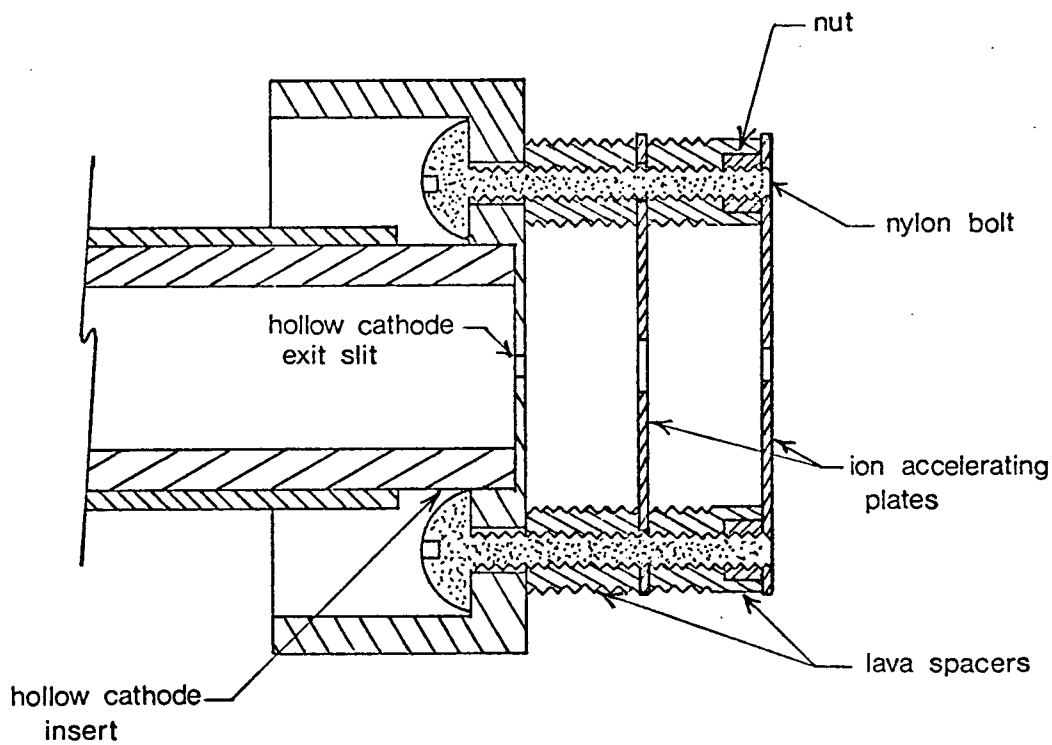

Figure 5. Ion Lens Assembly

The slits in all three plates were cut using a spark erosion cutter running at slow speed to keep the

edges of the slits from becoming ragged. The dimensions of the hollow cathode exit slit, centre slit, and final slit are respectively, .014 x .100 in, .040 x .160 in, and .030 x .150 in. The high tension leads were fixed to the centre and final plates by laying the wire at the edge of the plate, wrapping nickel foil around it and over a small section on both sides of the plate, and spot welding the wire to the nickel foil and the nickel to the stainless steel plate. Before installation, the plates were polished with #600 emery paper, 4/0 emery polishing paper, and a metal polish.

2.1.3 Stark Field Plates

The main criterion in the design of the high field region was to keep the distance between all exposed high voltage metal parts and grounded parts as small as possible, thereby keeping the breakdown voltage between them high. The Stark field plates in position in the high field region are shown in the two views of Fig. 6.

The grounded plate is bolted to a platform and the negative high voltage plate is supported from it by three steel pins. The pins are fixed to the grounded plate with set screws and slide in holes in lava pieces bolted to the negative plate. The fourth support is left out to allow a clear view of the ion beam where it enters the region

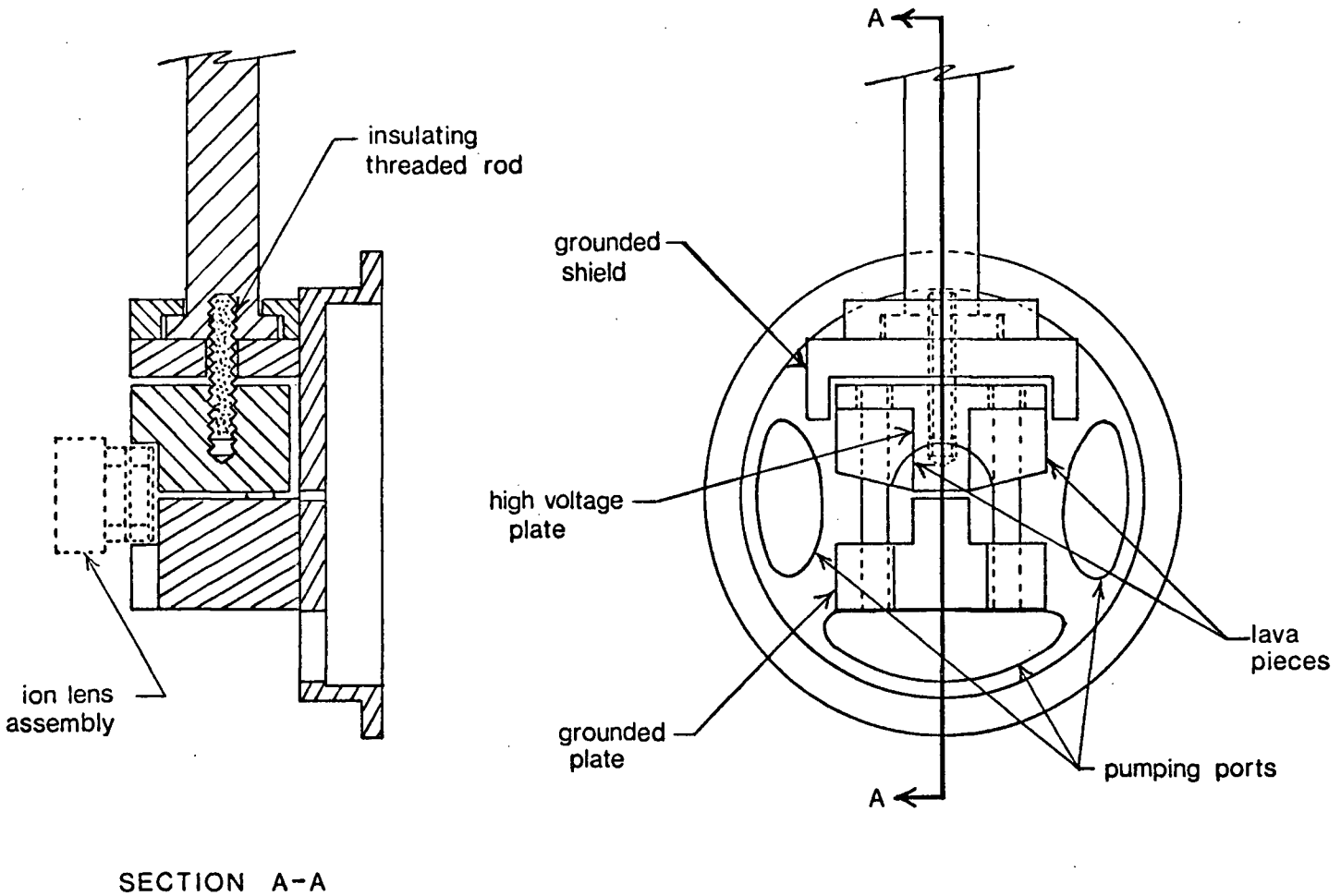

Figure 6. Detailed Assembly of Stark Field Plates

between the two plates. Behind the negative plate is a grounded aluminum shield which serves a dual purpose: one is to keep the distance from the back of the negative plate to the nearest grounded object small, and the other is to support the mechanism for moving the negative plate. This mechanism consists of an insulating threaded rod which is kept fixed in position (from the back of the support) and is turned in a tapped hole in the negative plate. Both the negative and grounded plates were machined out of the same piece of aluminum and cut apart only after the lava pieces had been attached and support holes drilled. This was done to ensure that the high field faces of both plates were as parallel as possible. The high voltage is fed to the negative plate by an insulated wire coming through the holes where the fourth pin would have been. On the end of the wire is a piece of brass which fits into the fourth hole in the negative plate and is held in by a set screw.

This whole assembly is contained in a brass housing with two viewing ports so that the beam between the high field plates can be viewed from both sides.

One further point concerning the high field region is worthy of note. The major problem in getting it operating properly was the prevention of breakdown from the final (8 kV) accelerating plate and the high voltage field

plate. One method used was to coat some of the exposed metal parts with a liquid porcelain called Sauereisen. The points where the wires attach to the accelerating plates and the steel support pins are two of the parts which were so coated. A lot of time was wasted using this technique until it was finally realized that the breakdown was being somehow enhanced by the Sauereisen (probably by outgassing from it). In the final version, the only material added to the field plate region was some vacuum epoxy (Ultra Torr) used to strengthen the junction points between the high voltage leads and the accelerating plates. The best breakdown prevention method was found to be careful polishing of all high voltage parts and attention to keeping the distances between them and grounded parts small.

2.1.4 Vacuum System

The system (see Fig. 7) is differentially pumped by a CVC MCF 300 diffusion pump (pumping speed 270 l/sec) and backed up by a Welch 1397 mechanical pump (pumping speed 7 l/sec). A liquid nitrogen cold trap and a butterfly valve separate the differential pump from the system, giving a pumping speed of about 100 l/sec at the valve. The conductance of the glass elbow to the system is about 250 l/sec (assuming molecular flow) giving a pumping

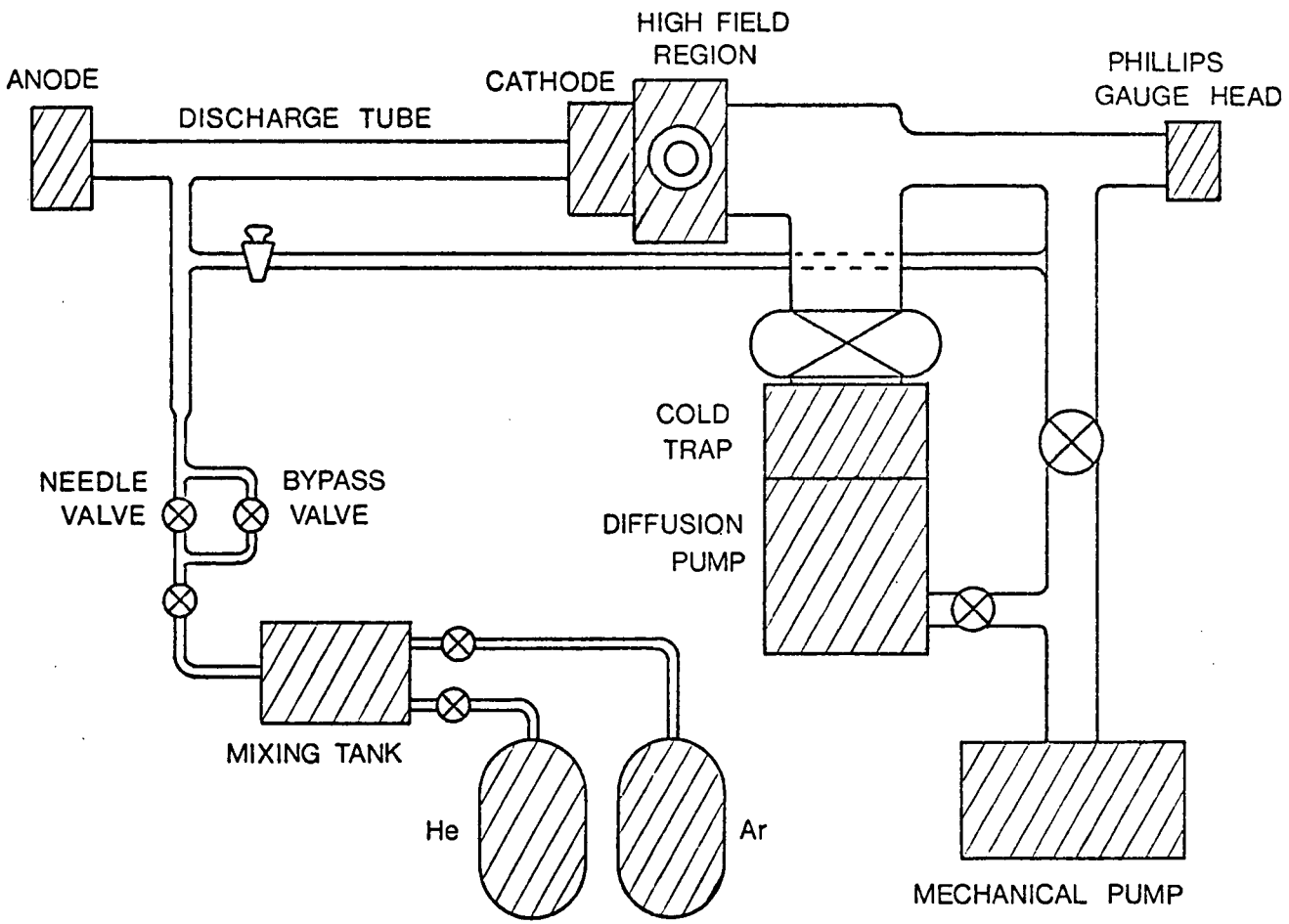

Figure 7. Vacuum System Schematic

speed at the outlet of the field plate region of about 70 l/sec. The number of ions in the field plate region increases very quickly with an increase in pressure in the discharge tube, but this, of course, increases the background pressure in the field plate region and the likelihood of high voltage breakdown. Thus the object of the pumping system is to maintain as large a pressure differential as possible between the discharge tube and the field plate region.

When running Ar in the system, it was necessary to mix in about one third He (by volume) to raise the breakdown voltage in the field plate region and to decrease sputtering of the cathode. The mixing of the two was done in a mixing tank at about atmospheric pressure. The gas flowed through a needle valve from this tank to the discharge tube.

One problem encountered in designing the vacuum system was a tendency for the discharge, especially at lower pressures, to go to the gas inlet needle valve or the discharge tube roughing line instead of to the hollow cathode. To prevent the discharge to the needle valve, a coil of poly - flo tubing about 1 m long was added to the gas inlet line and to prevent its going to the roughing line, a glass stopcock was placed between the discharge tube and the metal roughing line. This valve was, of course, closed

during an experimental run.

2.2 Data Acquisition System

The data acquisition system (see Fig. 8) consists of three main parts:

(i) an optical section consisting of a simple lens system and a monochromator with two exit slits;

(ii) a linear transmission wedge behind one slit; and

(iii) a photon counting electronics system to measure the intensities at both exit slits.

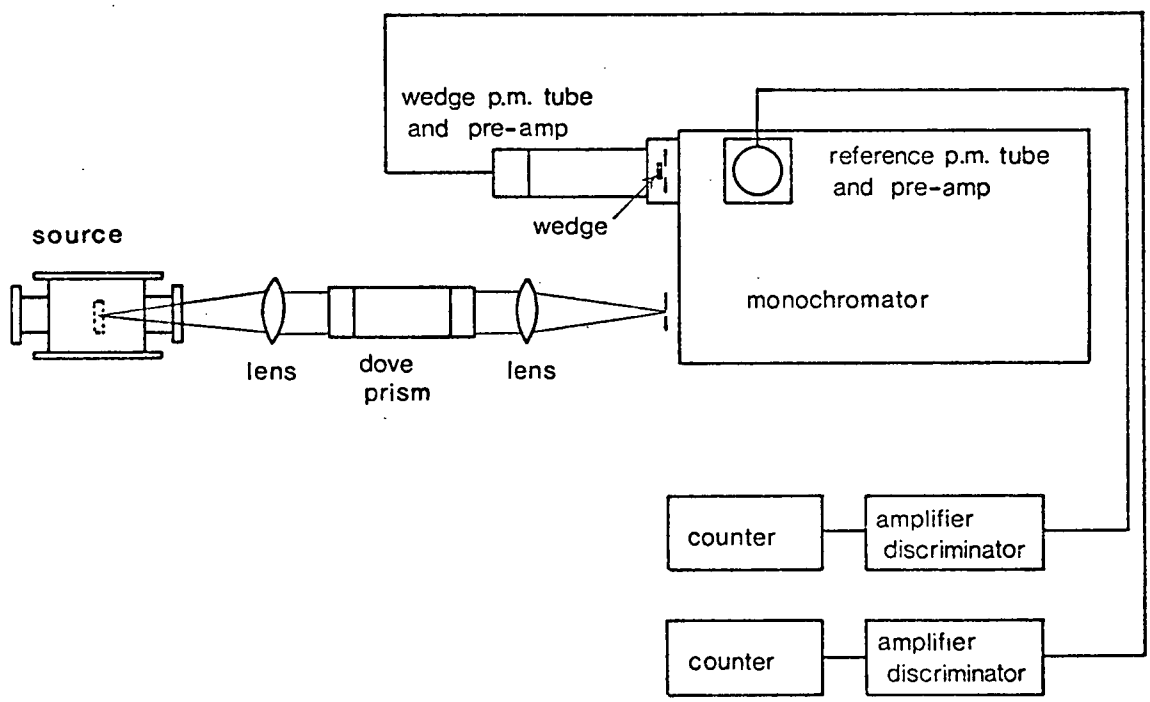

Figure 8. Data Acquisition System Block Diagram

2.2.1 Optical System

The lens system used consists of an objective lens of focal length 195 mm and diameter 36 mm placed such that the centre of the ion beam lies at its focal length and an imaging lens of focal length 178 mm and diameter 34 mm to image the parallel light from the first lens on the entrance slit of the monochromator. This lens matches the f-number (f 6.8) of the monochromator and the Stark source was designed to have approximately the same f-number. Between the two lenses is a dove prism to rotate the horizontal image from the ion beam into the vertical plane of the monochromator entrance slit.

The monchromator is a Spex 1702 3/4 metre instrument with a Bausch and Lomb grating blazed at 1 μm and having 1200 lines per mm. The resolution of the instrument is .030 A^{o} in third order with 6 μm slits. The monochromator is also equipped with a motor driven scan with scan speeds from .5 A^{o}/min to 5000 A^{o}/min.

For this experiment the monochromator was modified by the addition of a camera tower mounted through the hole provided in the top of the cover. A partially silvered mirror splits the beam into two parts sending part to the original Spex exit slit mounted on the top of the camera tower and the rest to a Hilger slit replacing the original

exit slit. The transmission wedge is mounted just behind this slit in a housing which allows it to be positioned properly with respect to the slit. The two exit slits were made parallel to the entrance slit and focussed by standard techniques.

2.2.2 Linear Transmission Wedge

The linear transmission wedge technique is described in full detail by Morris (1972). A short account of the production and use of the wedge is included here for completeness.

First a general description of the technique is in order. A neutral density filter whose transmission varies linearly from 0 to 1.0 over the width of the line (including most of the line wings) is placed in the exit plane of a monochromator and the exit slit is opened to the width of this "wedge". The transmission of the combined wedge and slit is shown in Fig. 9. The line whose shift is to be measured is placed in the centre of the wedge. When the line is shifted (in this experiment by application of an electric field), the shift in position of the line is translated into a change in intensity of the light transmitted by the wedge. As shown in Fig. 9, the shift of the line is small compared to the line width which in this

experiment is the instrument width. Shifts which could not be resolved simply by using the monochromator can be resolved using the transmission wedge.

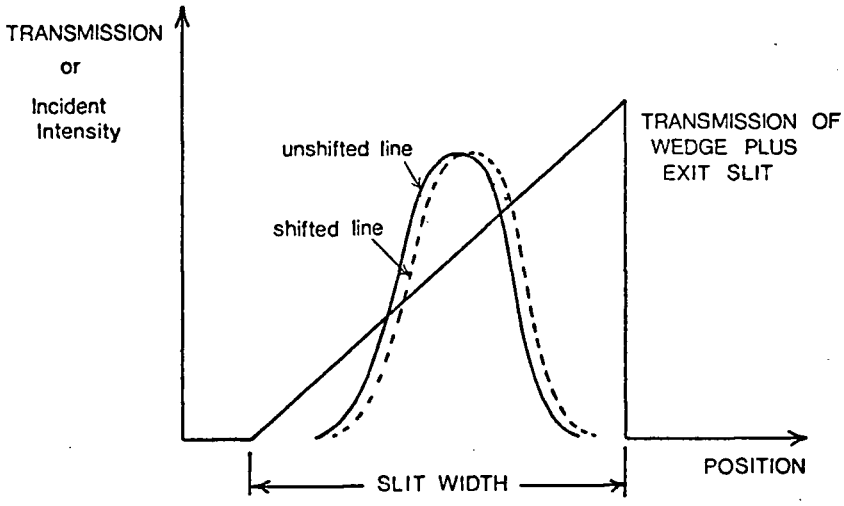

Figure 9. Ideal Transmission Wedge and Slit Profile

A perfectly linear transmission wedge would be very difficult to produce, but a good approximation can be made as follows: a fine grain spectroscopic plate (Kodak 649 F) was exposed to an extended light source with a knife edge between the plate and the source (see Fig. 10).

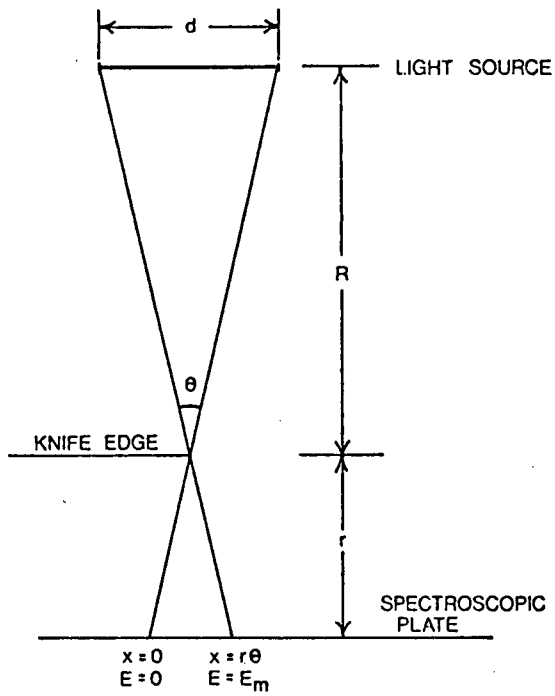

Figure 10. Wedge Production Schematic

At an arbitrary position x between x = 0 and x = rθ, the exposure is

$$E = \frac{x}{r\theta} E_m = \left(\frac{E_m R}{d\, r}\right) x$$

so that the exposure varies linearly with position. By changing the exposure time and the developer strength and developing time (thereby changing the slope and shape of the H and D curve of the plate), this linear exposure function was made into an approximately linear transmission function. This was done simply by trial and error: many exposures were made and different developer strengths and

times used. The plates produced were then scanned using a microdensitometer and the best one selected.

The width of the wedge desired is dictated by the instrument width which in this experiment (using a 20 μm entrance slit) was about 40 μm or .21 A^{O} in second order. This was determined experimentally by scanning the He I 3889 A^{O} Geissler line using 20 μm entrance and exit slits and using half the width of the profile at one tenth maximum. The wedge used is approximately linear from T = .80 to T = .25 and the length of this portion is about 100 μm or .5 A^{O} in second order. The values of the parameters used in the production of this wedge were:

d = 1.625 in

R = 15 in

r = .25 in

Exposure: 6 sec to a 60 W bulb behind a ground glass screen

Developer: Kodak D-19 diluted with 2 parts water

Developing time: 3 min

The wedge was mounted a few thousandths of an inch behind the exit slit in a special housing. The wedge was supported from the bottom and could be rotated about this lower pivot point by a differential screw attached to the top. This means of support allowed the wedge to be aligned

parallel to the exit slit. The aluminum plate on which the wedge was mounted could be positioned accurately behind the exit slit using a 2 in barrel micrometer screw.

The alignment of the wedge and reference slits was done by scanning the He I 3889 A^{o} Geissler line across the slits at 5 A^{o}/min and averaging the amplified and discriminated photon pulses to give an analog signal which was fed to a Hewlett - Packard 7034 A XY plotter (see next section). The optimum wedge position and slit width were determined by many scans with different slit widths and wedge positions until the best profile was obtained. The wedge and reference profiles finally used are shown in Fig. 11. The reference slit width was chosen because the

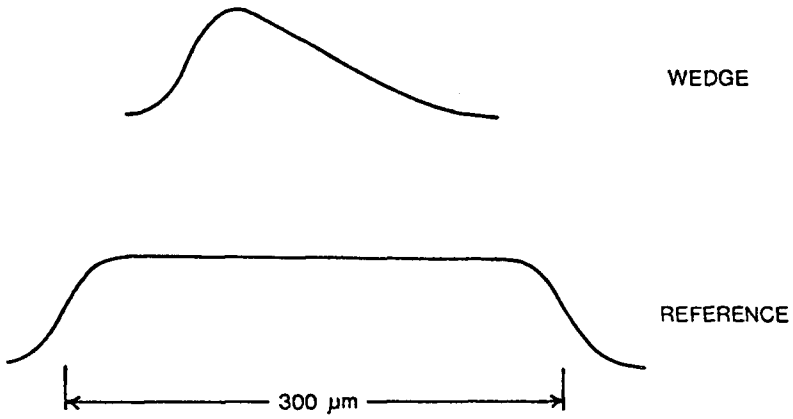

Figure 11. Experimental Wedge and Reference Profiles

slit edges tended to frost up when the photomultiplier

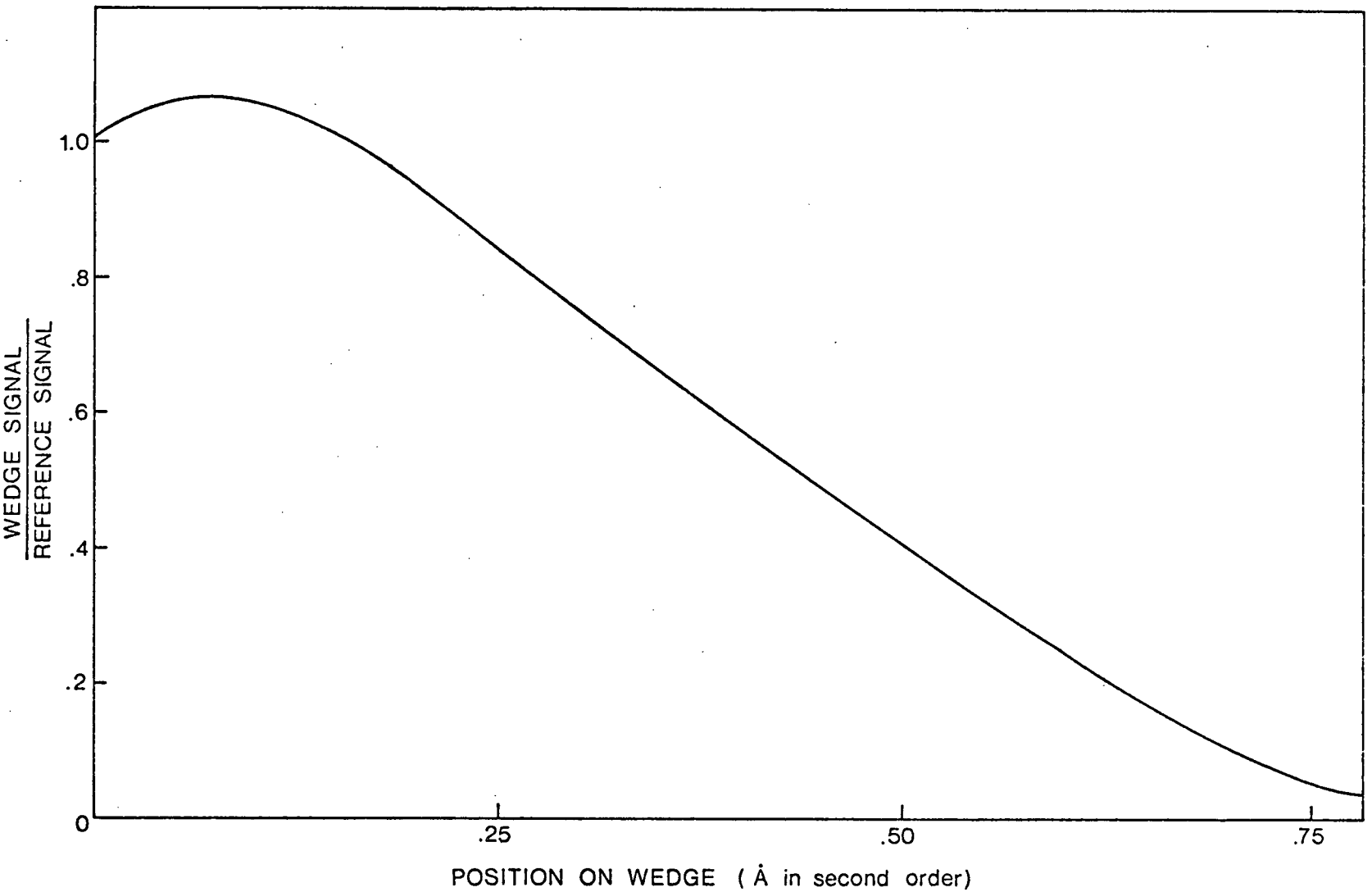

Figure 12. Wedge Calibration Curve

tubes were cooled. (This problem is described more fully in section 4.3).

The final wedge calibration was done by scanning the 3889 A^{o} He Geissler line very slowly (.5 A^{o}/min) across the slit and counting with both counters gated on for 1 sec at intervals of 10 sec by the circuitry described in the next section. The calibration curve is shown in Fig. 12.

2.2.3 Electronics

The electronics consists of two identical systems, one for each exit slit. Each system has one dry ice cooled photomultiplier tube, a photon pulse pre-amplifier contained in the photomultiplier tube housing, a pulse amplifier - discriminator, and a counter. (See Fig. 13).

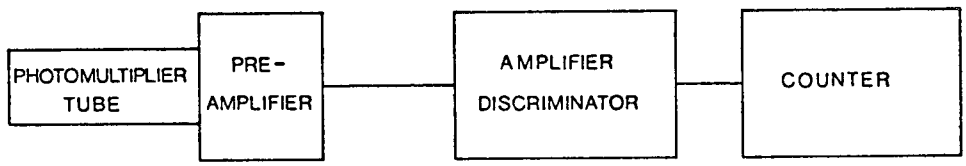

Figure 13. Electronics Schematic

The photomultiplier tubes are EMI 9558 B's having S - 20 photocathodes, risetimes of about 15 nsec and fairly low dark currents. Since the signal strength in this experiment was so low, special consideration was given to minimizing the dark current.

Several techniques were used. The first is the standard technique of placing an electrostatic shield at cathode potential around the tube against the glass. The tube was also washed in lukewarm water to remove all skin oils and other dirt; during and after a thorough rinsing, it was not touched directly with the hands. The resistors in the dynode chain of the tube were chosen to limit the chain current to about 150 μA because no more is needed for photon counting while any larger current generates heat in the tube housing, increasing the dark current. The metal photomultiplier tube housing was surrounded by a PVC cylindrical tube and the annulus between the two was filled with crushed dry ice to cool the tube to below -40° C. The dry ice container was made fairly air tight so that the evaporation of the CO_2 created a positive pressure in it. This was used to blow evaporated cold CO_2 into the photomultiplier tube housing from the back, thus cooling it faster and also preventing fogging of the photocathode window.

The photomultiplier pre-amplifier (Fig. 14) is

needed to give the current and voltage gain required to feed the 50Ω cable to the amplifier-discriminator circuit. The circuit is a modified version of one use previously by Camm (private communication). The anode signal is fed directly to the base of the first transistor of a two transistor negative feedback amplifier providing both current and voltage gain. The negative feedback gives the circuit a low input impedance (a few ohms), thus enabling it to follow very fast pulses. From the emitter of the second transistor the pulse enters an emitter follower to provide

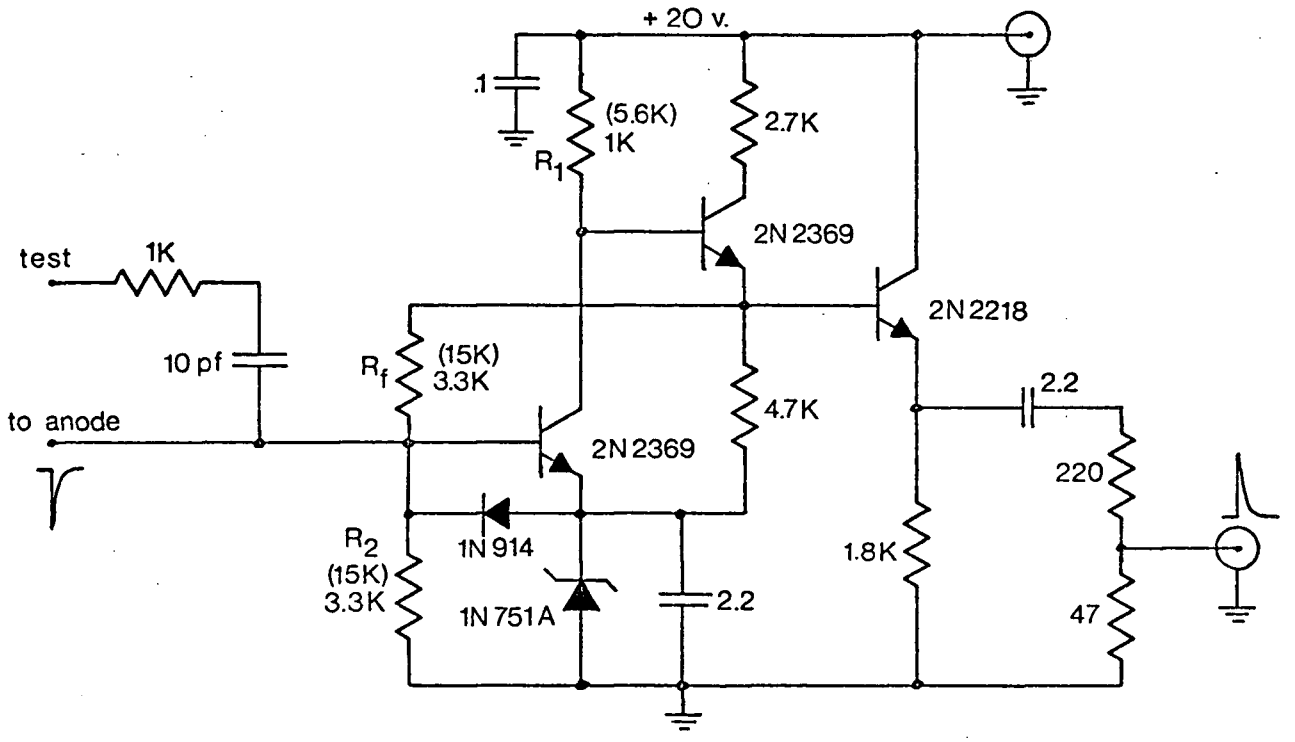

Figure 14. Photomultiplier Tube Pre-amplifier Circuit

more current gain. In this experiment, the output pulse was capacitively coupled to a voltage dividing network consisting of a 220Ω and a 47Ω resistor in series. This network was required to cut down the overall voltage gain to avoid saturating the input amplifier of the amplifier-discriminator circuit.

The two modifications made to the circuit for this experiment were to change the gain and to change the test input to simulate a photomultiplier tube source.

The gain of the pre-amp is proportional to the value of R_f, the feedback resistor (Fig. 14). R_f was decreased from 15 KΩ to the present value of 3.3 KΩ, decreasing the gain by a factor of about 4.5. To maintain the proper bias levels in the first two transistor , the values of R_1 and R_2 had to be changed by the same proportion.

Because of the low input impedance of the circuit, the photomultiplier tube current pulses at the input are not visible using present oscilloscopes. For this reason, a test input was provided. The input consists of a differentiating network (the 10 pf capacitor and the "few ohm" input impedance of the circuit) plus a series 1KΩ resistor. This 1KΩ resistor determines the time in which the current pulse is injected into the base of the input transistor. With a capacitance of 10 pf, an input pulse

of 100 - 200 mV gives a current pulse of 10^7 electrons in about 15 nsec to the base of the input transistor. This simulates closely a single photon pulse from the photomultiplier tube.

From the photomultiplier tube housing, the pulse was fed via a 50Ω cable to the amplifier-discriminator circuit (see Fig. 15).* The input amplifier is an MC 1445 wideband amplifier IC with a voltage gain of 10 and a maximum output pulse of 500 mV. The inverted output pulse is fed to the inverting input of an MC 1710C differential comparator IC. This circuit operates in a similar manner to a Schmitt trigger. When the input pulse becomes more negative than the negative reference voltage dialed on the 500Ω potentiometer, the output goes from a low to a high state and remains high for a time determined by the RC series feedback network (providing the input pulse is short compared with this time). Thus the MC 1710C acts as a voltage discriminator, giving a standard 40 nsec, 1.5 V output pulse for every input pulse over the threshold level. From the comparator, the pulse goes through a Darlington pair emitter follower and into the 50 Ω cable to the counters.

At the comparator output there is also an averaging network to provide an analog output to operate the XY plotter.

* The idea for the design of the discriminator section of this circuit was obtained from a colleague at ISAS, U. of S., Saskatoon. The design itself was done partly at U. of S. and partly at U.B.C.

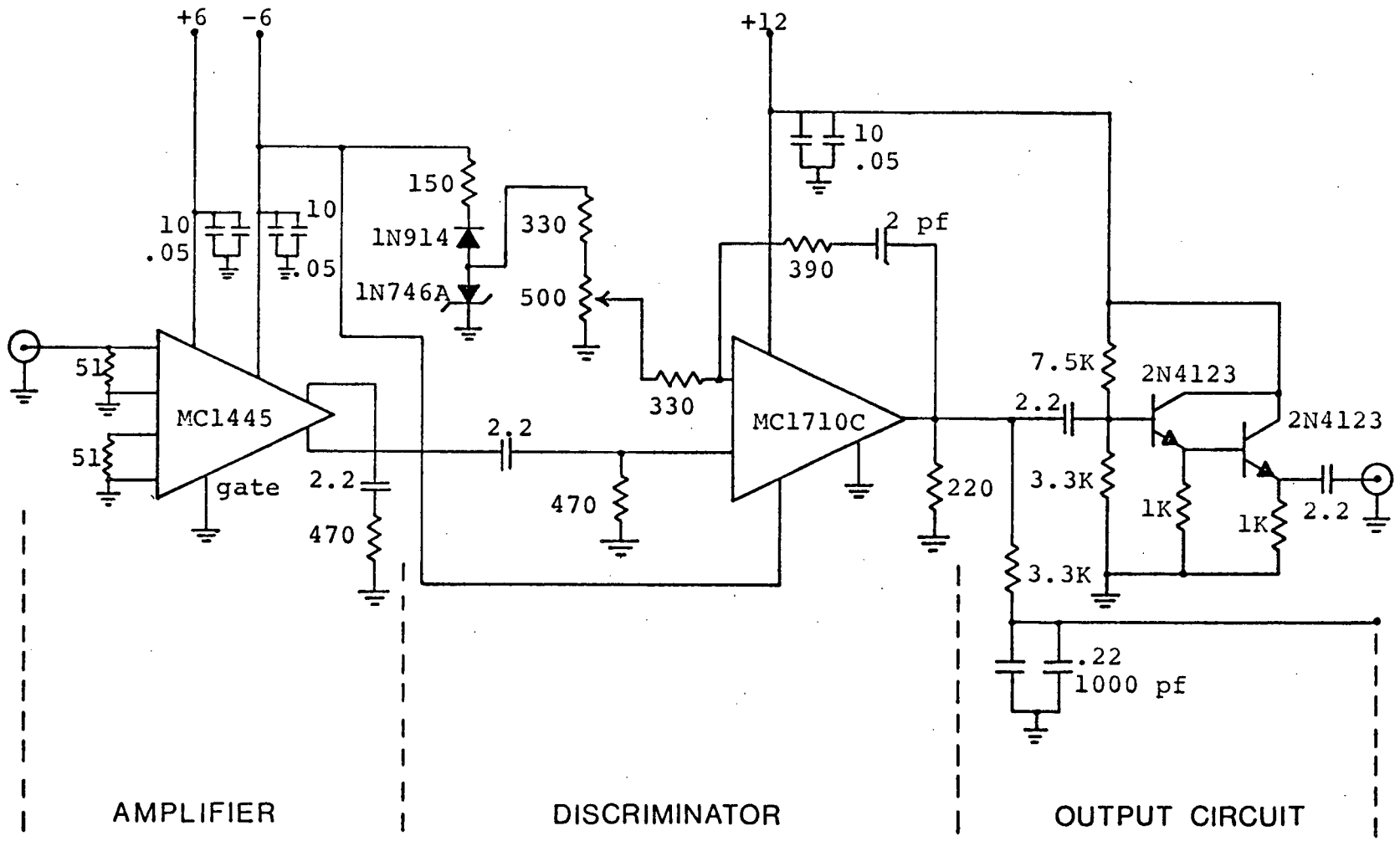

Figure 15. Photon Pulse Amplifier Discriminator Circuit

It consists of a low pass filter formed by a 3.3 KΩ resistor in series with a .22 μf and 1000 pf capacitor network.

The two counters are 40 MHz Analog Digital Research CM 40A's which have been modified slightly to enable them to be gated simultaneously and for long integration times. The modifications are shown in Fig. 16.

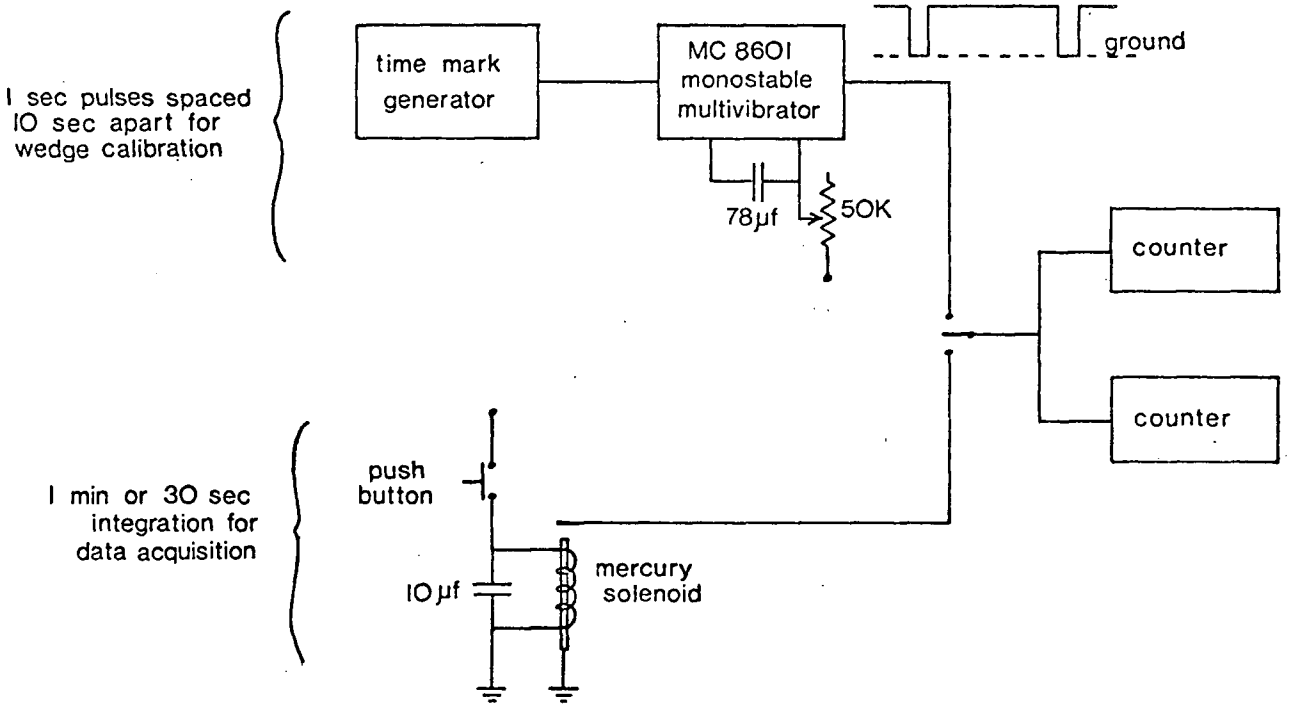

Figure 16. Counter Modifications

Both modifications consist of altering the totalize function of the counters. Normally, placing the counter function switch to totalize grounds the counter gate, allowing pulses to be counted while it remains grounded.

In the modified counters, instead of going to the function switch, the counter gates are brought to a double throw switch enabling them to be controlled externally in two ways.

One switch position connects the counter gates to a mercury solenoid switch controlled by a push button. When the button is pushed, both counter gates are grounded and the counters count until the button is released. This method was used in the 1 min and 30 sec integration times required in the Stark data gathering.

The other switch position connects the counter gates to the output of an MC 8601 monostable multivibrator which, when hit by a pulse from the time mark generator, grounds the counter gates for a time determined by the external RC constant chosen. This method of gating the counters was used for obtaining the wedge calibration profile. The He I 3889 A^{O} Geissler line was scanned across the wedge at a rate of .5 A^{O}/min and the time-mark generator - multivibrator circuitry triggered the counters for 1 sec at 10 sec intervals.

The response of the monochromator plus electronics was observed to be linear up to a count rate of about 350 KHz. At a rate of 400 KHz, the error due to non-linear response was about 3% (Fig. 17). Above 400 KHz the error due to

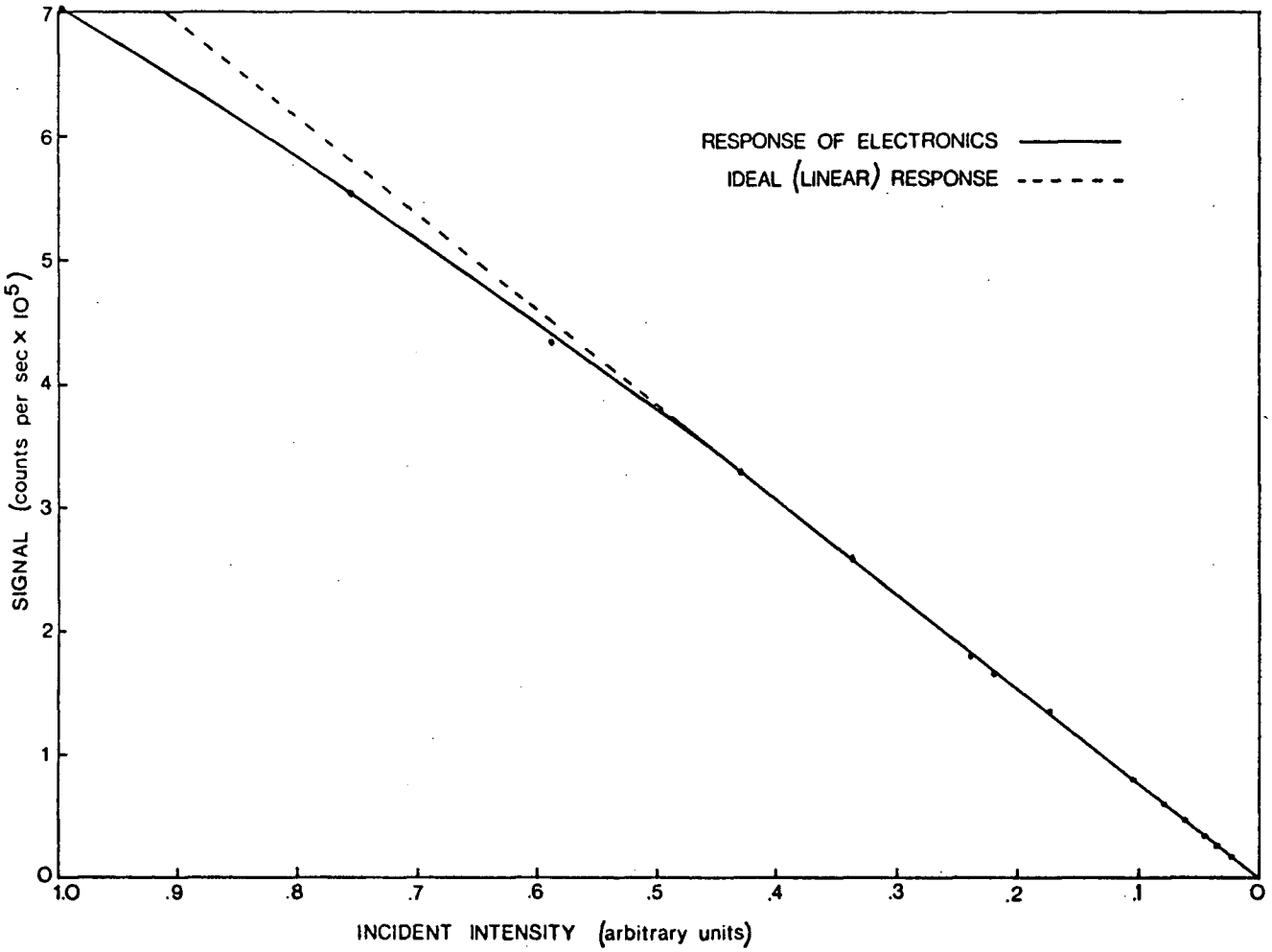

Figure 17. Response Curve of Photon Counting Electronics

non-linearity is considerable. This non-linearity at high count rates results from two factors.

The first is pulse pile-up. With a discriminator output pulse width of about 45 nsec, the pulse pair resolution of the circuit was 80 nsec. Therefore if two pulses arrive within 80 nsec of one another only one of them is counted. The probability of this happening follows the negative exponential distribution (assuming the pulses are random and hence follow Poisson statistics). At a 400 KHz count rate and 80 nsec dead time this probability is 3 %.

The second factor is the shift of the pulse base line at high count rates. The circuitry used is all a.c. coupled and the effect of the coupling capacitors is to cause the output pulses from them to have a mean value of zero volts. Thus when the pulse rate increases, the baseline shifts down, decreasing the peak pulse voltage and therefore effectively increasing the discriminator voltage. So if the pulse rate goes up by a certain percentage, the count rate (number of pulses through the discriminator) goes up by a smaller percentage. This effect becomes noticeable at about 500 KHz count rates.

In this experiment, the data count rates were much less than 350 KHz and during wedge calibrations the Geissler tube voltage was decreased until the He I 3889 A^{o} line gave a count rate of less than 350 KHz.

Chapter Three

EXPERIMENTAL PROCEDURE

In this chapter the data gathering procedure (as opposed to the setting up procedures) is described. In the first two sections, dealing with the Stark source and the optical system, only special procedures are detailed, as the rest is self-explanatory after reading Chapter Two. More detail is given in the data gathering and calculations sections (3.3 and 3.4, respectively).

3.1 Stark Source

Before setting the gas flow, the ion lens accelerating voltages, and the field plate voltage at their operating values, an "electrode conditioning" procedure was necessary. First the needle valve from the mixing tank was opened to about two thirds of its operating value and the glow discharge started. The centre and final accelerating plates of the ion lens were then raised to -.75 kV and -4 kV. After about 10 min these voltages could be raised to their

operating values of -1.5 kV and -8 kV respectively and over about the next half hour, the mixing tank needle valve could be opened to its operating aperture. (This term, "operating aperture", though it sounds very official, is arrived at completely empirically. It is the maximum needle valve setting which doesn't produce sparking in the field plate region). The length of time required for this "electrode conditioning" is shorter if the source has been used often in the previous week or so and a good deal longer if the source is being run for the first time after being at atmospheric in air.

3.1 Optical Alignment

Before each experimental run, the alignment of the optics was checked.* The check was done by removing the wedge photomultiplier tube and shining a 650 W Quartz lamp backwards through the monochromator. (This method was preferred over laser line-up techniques because, with the laser, care must be taken that the beam hits the centre of the mirrors and grating in the monochromator and because the laser gives no information on the focus of the system). The image of the slit was seen between the Stark field plates and its position adjusted by raising or lowering the lens

* The reason for this is that the time taken to do the check is only a few minutes whereas, if the monochromator or source had been inadvertently knocked out of alignment and not realigned, a whole day of data gathering would be wasted.

nearest the source. The focus was checked by the method of parallax. The final focussing was done by looking at the image of the beam on the entrance slit of the monochromator and the final positioning of the image was done by raising or lowering the objective lens to maximize the count rate of one of the spectral lines of the gas being used.

3.3 Data Acquisition

Once the source was operating, the optical alignment checked, and the photomultiplier tubes cooled, data could be taken. First the line to be studied was positioned on the wedge by noting the maximum wedge signal and scanning the line across the wedge until this signal was cut in half. Zero field readings of both total signals and dark currents were then taken. Without touching the monochromator scan, -2 kV and -5 kV readings were taken. With the Ar-He mixture at each Stark voltage setting, dark current and total signal (i.e. signal plus dark current) readings were alternated. Usually 4 dark current and 3 total signal readings were taken. When He alone was run, the dark current was usually stable enough that only one reading of dark current and one of the signal was required. The count integration time was usually 1 min but was lowered to 30 sec if the signal was unusually strong.

To calibrate the electric field at the two voltage

settings and to check that the apparatus was working properly, the shifts of a few isolated lines of He I were measured. The lines chosen were 5016 A^{o}, 7281 A^{o}, 6678 A^{o}, and 3889 A^{o}. The first three were done in first order and the last in second order. To check for repeatability, 5016 A^{o} was repeated, this time in second order, and 3889 A^{o} was repeated, again in second order.

The Ar-He mixture was then run and the shifts of the following lines were measured: Ar I 4266 A^{o} and 4272 A^{o}, Ar II 4727 A^{o} and 4806 A^{o}, He 3889 A^{o}. All were measured in second order. The measurements were repeated with Ar I 4266 A^{o} and 4272 A^{o}, Ar II 4727 A^{o}. The other two plus He I 5016 A^{o} and 6678 A^{o} would also have been measured in the second run, but at this point, the lava spacers in the ion lens began to track and no further data could be taken.

3.4 Calculations

The total signals and dark currents obtained for each line were averaged and the net signals calculated. The ratio of wedge signal to reference signal was calculated for each voltage setting. The problem then arose that the zero field ratios (the ratios with the line simply placed in the middle of the wedge) were not equal for the different lines. This was attributed to the differences in polarization of the different lines and the different light throughputs

from entrance slit to wedge slit and entrance slit to reference slit for different polarizations.

To get around this problem the signal ratios for 2 and 5 kV were subtracted from that for zero field and the differences were expressed as percentages of the zero field ratio. The equivalent shifts on the calibration curve were calculated by multiplying these percentages by the ratio at the half way point of the wedge calibration curve. The corresponding wavelength shifts could then be read off the calibration curve or calculated using the slope of the curve. Both methods were used for comparison. Table 1 shows the shifts obtained from the graph and from the slope and also the "experimental shift". This "experimental shift" is a combination of the shift from the graph and the shift from the slope. If the shift was less than .06 A^{o}, the shift from the slope was taken as the experimental shift and if the shift was greater than .06 A^{o}, the shift from the graph was taken as the experimental shift.

Table 2 shows how the shifts obtained in this experiment compare with previous experimental values and with theore tical values (calculated in the Coulomb approximation by A.J. Barnard). The previous experimental values were scaled quadratically to the fields used in this experiment.

Table 1. Experimental Shifts

LINE	STARK VOLTAGE (kV)	SHIFT (FROM GRAPH) (A^{o})	SHIFT (FROM SLOPE) (A^{o})	SHIFT (ADOPTED VALUE) (A^{o})
He I	2	-.038	-.038	-.038
5016 A^{o}	5	-.263	-.248	-.263
He I	2	.034	.032	.032
7281 A^{o}	5	.116	.107	.116
He I	2	.056	.051	.051
6678 A^{o}	5	.265	.264	.265
He I	2	.028	.027	.027
3389 A^{o}	5	.070	.067	.070
Ar I	2	.020	.018	.018
4266 A^{o}	5	.051	.049	.049
Ar I	2	.019	.019	.019
4272 A^{o}	5	.034	.034	.034
Ar II	2	.002	.001	.001
4727 A^{o}	5	.010	.010	.010
Ar II	2	.007	.005	.005
4806 A^{o}	5	.009	.009	.009

Table 2. Comparison of measured shifts with previous experiments and with theoretical values

LINE	FIELD (kV/cm)	SHIFTS (A^o)		
		This Experiment	Previous Experiments	Theoretical
He I 7281 A^o	19.2	.032	--	.014
	50.5	.116	--	.095
He I 6678 A^o	19.2	.051	--	.039
	50.5	.265	--	..273
He I 3889 A^o	19.2	.027	.004 LB	.004
	50.5	.070	.031 LB	.027
Ar I 4266 A^o	19.2	.018	.004 M1	--
	50.5	.049	.029 M1	--
Ar I 4272 A^o	19.2	.019	.003 M1	--
	50.5	.034	.014 M1	--
Ar II 4727 A^o	19.2	.001	.00 M2	$-.055 \times 10^{-3}$
	50.5	.010	.00 M2	$-.38 \times 10^{-3}$
Ar II 4806 A^o	19.2	.005	.00 M2	$-.066 \times 10^{-3}$
	50.5	.009	.00 M2	$-.46 \times 10^{-3}$

LB Landolt-Boernstein (1950)
M1 Minnhagen (1949)
M2 Minnhagen (1948)

Chapter Four

CONCLUSIONS

4.1 Introduction

As seen in Table 2, the shifts obtained in this experiment agree with those calculated or measured previously only to within about .02 A^{o} for He and .03 A^{o} for Ar. If we assume that the only source of error is the Poisson noise of the photons incident on the photomultiplier tubes, the accuracy should be .003 A^{o} for the He I lines and .01 A^{o} for the Ar I and Ar II lines. This leads to the conclusion that there must be other sources of error.

These sources of error were easily recognized during the experiment and the improvements required to correct them are quite straightforward. There was no time to carry out these improvements for this experiment but they should certainly be made before attempting any further work.

In the following sections, the sources of error and improvements which could be made to reduce them are discussed. Concluding remarks are made in the last section.

4.2 Problems with Stark Source

The major source of error can be seen by examining the dark current data. This data shows an increase in the "apparent" dark current when the Stark voltage was increased and a higher dark current for the Ar-He mixture than for straight He gas. The increase in dark noise was due to r.f. noise produced by low current sparking in the Stark source. These low current breakdowns were visible in the source and the r.f. noise produced by them could be seen on the 50 Ω cables from the photomultiplier tube pre-amps (with the aid of a Tektronix 585 oscilloscope).

There are two improvements which would eliminate this problem. Both consist of decreasing the background pressure in the field plate region thus increasing the breakdown voltage. The obvious way to do this would be to decrease the discharge tube pressure, but this would also decrease the number of ions produced. The goal, then, is not just to decrease the field plate region pressure, but to increase the pressure differential between the discharge tube and the field plate region.

The first improvement is the simplest and most obvious: use a faster diffusion pump and increase the size of the pumping line to the field plate region.

The second is more complicated: instead of just

one stage of differential pumping, use two stages. The Stark source apparatus would then consist of three separate sections: the high pressure (a few Torr) hollow cathode discharge region; a second region containing only the slit at the botom of the hollow cathode and an ion accelerating lens; and a third region joined to the second by a small slit and containing a second ion lens and the Stark field plates. The second and third regions would each have its own diffusion pump system, resulting in a much lower pressure in the field plate region.

If the pressure differential between the hollow cathode discharge region and the field plate region were increased by either of the two methods mentioned above, a higher pressure could be tolerated in the discharge tube. This would lead to the production of more ions in the hollow cathode and the ion signal would increase, enabling one to use a narrower monochromator slit width. The resulting narrower instrument profile would allow one to use a steeper wedge and hence the small ion line shifts would be easier to measure.

A second problem with the present Stark source is that the ion beam gets only about 2 mm into the high field region before being dragged to the negative plate. Thus at least half of the beam lies in the non-uniform fringe field of the plates and cannot be used for measurement. This

problem could be partly overcome by using the two stage differential pumping system described in the last section. Because the field plate region in this system would have a very low background pressure, the final accelerating plate voltage and hence the velocity with which the ions are shot into the high field region could be increased. Thus they would travel further into the region before hitting the negative plate.

4.3 Problems with Data Acquisition System

Another major source of error was the fact that, after running for an hour or so, the edges of both exit slits and the surface of the wedge became partially frosted, thus changing the slope and width of the wedge. In this experiment, the frost was partially cleared off the reference slit by stroking a pipe cleaner across it periodically. However, this is at best a clumsy solution and certainly does nothing for the wedge and wedge slit.

This problem could be eliminated through use of a properly designed hermetically sealed dry ice cooled photomultiplier tube housing. These are available commercially.

Improvements could also be made in the photomultiplier tubes themselves. The dark current data taken shows that one photomultiplier tube had a much higher dark current than

the other and that both had fairly high dark currents even at dry ice temperatures. There are tubes available with inherently lower dark currents than the EMI 9558B or lower dark currents achieved by restricting the photocathode surface. It is also possible to have tubes of a particular type selected for low dark current.

4.4 Data Handling Improvements

Several improvements could be made to the data acquisition system which would increase both its accuracy and efficiency.

The dark noise fluctuations caused by the r.f. noise from the Stark source were a problem mainly because they were on a time scale of the order of the integration time. The accuracy of the data taken could by improved even in the face of this r.f. noise by chopping the light into the monochromator at a few hundred Hertz. The output from the photomultiplier tubes would then alternate between total signal and dark current at a rate much faster than the r.f. noise fluctuations. This signal could be easily demodulated to feed the total signal and dark current to different counters.

Once the accuracy of the experiment has been improved, the Stark shifts of large numbers of lines of

many elements and ions can be measured using this technique. Without some automation of the data acquisition, this could be extremely tedious. In the automated system, data could be transferred from the counters to magnetic tape at the push of a button and the intensity changes could be translated into line shifts by a computer using a wedge calibration curve previously fed into it.

4.5 Alternative Method of Measurement

Once the problems of frost on the slits and wedge, spurious and fluctuating dark currents, etc. are solved, the wedge technique should be able to measure shifts to an accuracy of .001 A^{o}. Before proceeding with the improvements detailed above, one should ask whether there is another, perhaps simpler, technique which can attain or surpass this accuracy. One such technique is the use of a Fabry-Perot etalon in series with a monochromator.

This method has a few advantages over the wedge technique. Its resolution can be .001 A^{o} or better, a number of lines can be measured at once, and, since a spectroscopic plate is used as a detector, the method is immune to the effects of r.f. noise from the Stark source.

Its major disadvantage is that it cuts down the intensity considerably and the intensity which does get

through is spread into numerous rings, leaving a very low flux for the plate to detect. This single disadvantage could render the Fabry-Perot technique useless in this experiment, but since it is simple to set up it is certainly worth a try in future work.

4.6 Concluding Remarks

After such a gloomy discussion of the myriad sources of error encountered, one might be tempted to question whether it is possible, even without these additional errors, to measure Stark shifts to an accuracy of .001 A^{o} using this technique. This question should certainly be pursued.

If we assume that improvements made in the apparatus allow us to close the entrance slit to 10 μm, we will have a line width of .05 A^{o}. It will probably be somewhat bigger than this, so the wedge will have to be .1 A^{o} wide. Take the maximum value for the wedge to reference signal ratio, s/S, to be 1 and consider the useable linear portion of the wedge to be from s/S = .25 to s/S = .85. To measure a change in wavelength of .001 A^{o} using this wedge we must measure the wedge and reference signals to an accuracy of .5%. To attain this accuracy with the only source of noise being Poisson noise, we must integrate until we have 90×10^{3} signal counts (with a signal to noise ratio of 10). With

the signal strengths encountered in this experiment, the integration time would have to be a few minutes. This length of time is certainly not unreasonable.

Thus we can conclude that an experiment incorporating the improvements outlined above should produce shift measurements of the required accuracy.

BIBLIOGRAPHY

Barnard, G.P., 1953, Modern Mass Spectrometry, London Institute of Physics.

Bonch-Bruevich, A.M. and V.A. Khodovoi, 1968, Sov. Phys. Uspekhi, 10, 637.

Condon, E.U. and G.H. Shortley, 1951, The Theory of Atomic Spectra, Cambridge U. Press.

Dushman, Saul, 1962, Scientific Foundations of Vacuum Technology, John Wiley.

Foster, J.S. and H. Snell, 1937, Proc. Lond. Phys. Soc. A, 162, 351.

Howatson, A.W., 1965, An Introduction to Gas Discharges, Pergamon Press, London.

Landolt-Boernstein, 1950, Zahlenwerte u. Funktionen, 1:1 Springer Verlag, Berlin.

Llewellyn-Jones, F., 1966, The Glow Discharge and an Introduction to Plasma Physics, Methuen and Co., London.

Maissel, L., 1958, J. Opt. Soc. Amer., 48 (11), 853.

Mark, H. and R. Wierl, 1929, Zeitschrift f. Physik, 53, 528.

Meyer, Paul L., 1966, Introductory Probability and Statistical Applications, Addison-Wesley.

Minnhagen, L., 1948, Arkiv f. Mat., Astr. o. Fysi k, 35A(16).

Minnhagen, L., 1949, Arkiv f. Fysik, 1(20), 425.

Minnhagen, L., 1963, Arkiv f. Fysik, 25, 203.

Morris, R.N., 1972, Ph.D. Thesis, University of B.C.

Ryde, N., 1932, Zeitschrift f. Physik, 77, 515.

Ryde, N., 1938, Zeitschrift f. Physik, 109, 108.

Ryde, N., 1941, Ark. f. Mat., Astr. o. Fysik, 28B(2).

Steubing, W. and J.A. Schaeder, 1936, J. Appl. Phys. 37(6), 2405.

Thornton, R.L., 1935, Proc. Lond. Phys. Soc. A, 150, 259.

Verleger, H., 1939, Ergebnisse der Exakten Naturwissenschaften, 18, 99.

Von Engel, A., 1965, Ionized Gases, Oxford U. Press.

Weston, G.F., Cold Cathode Glow Discharges, Iliffe Books Ltd., London.

Zatzick, M.R., 1970, "Applying Digital Techniques to Photon Counting", Research and Development, Nov., 1970.

Zatzick, M.R., "Photomultiplier Tube Selection and Housing Design for Wideband Photon Counting", Applications Note 71021, S.S.R. Instruments Co.